EGG-M-92498
CONF-9210204--3

NATURAL CIRCULATION UNDER SEVERE ACCIDENT CONDITIONS[a]

D. J. Pafford V. X. Tung[b]
D. J. Hanson S. V. Chmielewski[c]

Idaho National Engineering Laboratory
EG&G Idaho Inc.

EGG-M--92498

DE93 005245

ABSTRACT

Research is being conducted to better understand natural circulation phenomena in mixtures of steam and noncondensibles and its influence on the temperature of the vessel internals and the hot leg, pressurizer surge line, and steam generator tubes. The temperature of these structures is important because their failure prior to reactor vessel lower head failure could reduce the likelihood of containment failure as a result of direct containment heating. Computer code calculations (MELPROG, SCDAP/RELAP5/MOD3) predict high fluid temperatures in the upper plenum resulting from in-vessel natural circulation. Using a simple model for the guide tube phenomena, high upper plenum temperatures are shown to be consistent with the relatively low temperatures that were deduced metallurgically from leadscrews removed from the TMI-2 upper plenum. Evaluation of the capabilities of the RELAP5/MOD3 computer code to predict natural circulation behavior was also performed. The code was used to model the Westinghouse natural circulation experimental facility. Comparisons between code calculations and results from experiments show good agreement.

1. INTRODUCTION

During the latter stages of severe accidents in pressurized water reactors (PWRs), the inventory in the reactor coolant system may be significantly depleted and cells of natural circulation may be established in the reactor vessel, hot legs, and steam generators. In the hot leg, hot steam, or a mixture of steam and hydrogen, flows from the vessel along the upper portion of the pipe and cooler fluid is returned to the vessel along the lower portion. After some mixing in the steam generator inlet plenum, fluid enters the steam generator tubes and exchanges energy with the tubes and the secondary fluid before returning to the inlet plenum and hot leg. The net

---

a. Work supported by the U. S. Nuclear Regulatory Commission, Office of Nuclear Regulatory Research under DOE Idaho Field Office Contract No. DE-AC07-76ID01570
b. Currently at Aerospace Corporation, El Segundo, California
c. Currently at Detroit Edison, Detroit, Michigan

result of these natural circulation flows is to transport energy from the core and distribute it in the upper plenum and ex-vessel structures. Such natural circulation flows have been observed experimentally [1,2] and predicted by severe accident computer codes such as SCDAP/RELAP5 [3] and MELPROG [4].

The phenomena associated with natural circulation of mixtures of steam and noncondensibles is being evaluated to better understand their influence on the temperature of the vessel internals and the ex-vessel structures including the hot leg, pressurizer surge line, and steam generator tubes. High temperature creep rupture failure of the ex-vessel structures prior to failure of the reactor vessel lower head has the potential to reduce the likelihood of containment failure as a result of direct containment heating. This paper provides results from studies that have been completed in two areas:

(a) The resolution of perceived inconsistencies between computerized code results and information on upper plenum temperatures obtained from the Three Mile Island, Unit 2 (TMI-2) accident

(b) An assessment of the capability RELAP5/MOD3 to calculate natural circulation through a comparison of calculated results with natural circulation experimental data.

The following sections describe the analysis performed and results for these two areas.

2. TMI-2 UPPER PLENUM TEMPERATURE RESPONSE

Analyses of the TMI-2 accident [4] or similar scenarios [3] predict periods of natural circulation in the upper plenum with fluid temperatures as high as 1800K. Moreover, the predicted fluid temperature shows little variation in either the axial or the radial directions. However, these predicted temperatures appear to be incongruent with the temperatures deduced by a metallurgical examination of the B8 and H8 leadscrews recovered from the upper plenum of TMI-2 [5]. As shown in Figure 1, these temperatures ranged from 666K to 1255K with the bottom of the leadscrews experiencing a much higher temperature than the top. Not only are these temperatures much lower than those predicted by the codes, but they could also be interpreted as an indication of the existence of some stratification in the upper plenum. Such stratification, however, has been discounted by earlier work performed in this program [6] which indicated that long-term hydrogen stratification in the reactor vessel is not likely due to turbulent mixing associated with high Rayleigh number natural convection. Mixing time scales were predicted to be short (a few minutes), even when a fully stratified starting condition was assumed.

Analysis Approach

An analysis was performed to examine inconsistencies between the leadscrew temperatures reported in Reference 5 and the fluid temperatures in the upper plenum reported in References 3 and 4. Several different mechanisms are examined to determine their influence on leadscrew temperatures. A bounding

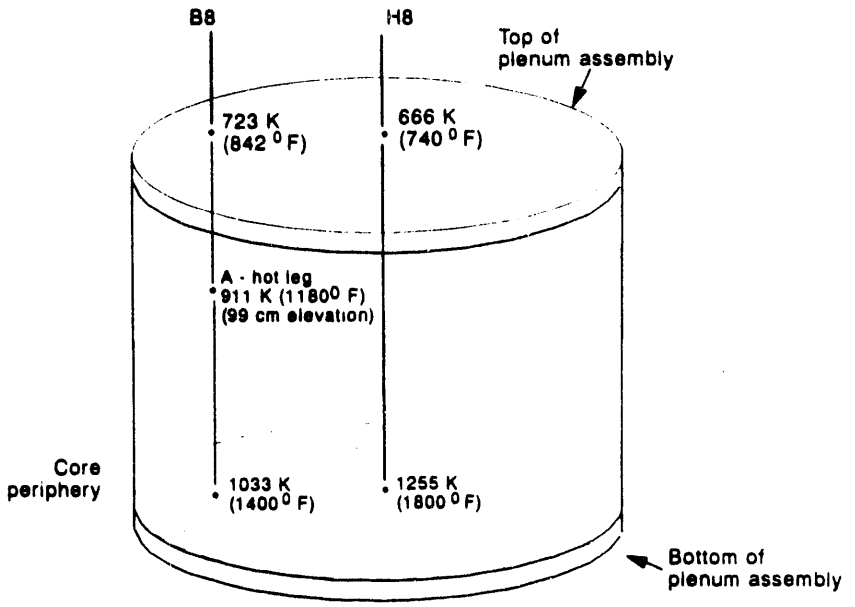

Figure 1. Results from metallurgical examination of TMI-2 leadscrews.

evaluation was performed initially to examine the influence of axial conduction along the lead screw and to assess the relative importance of radiation inside the tube. Results from these analyses indicated that axial conduction was not a significant influence, but radiation heat transfer must be considered in evaluating the leadscrew temperature. Based on these results, it was hypothesized that the guide tube provides an intervening shield between the leadscrew and the relatively hot fluid in the upper plenum. Initially, the outside surface of the guide tube was heated (via a combination of both radiation and convection) by the hot fluid in the upper plenum. Subsequently, the temperature difference between the guide tube and the leadscrew set up a convective current which serves as a heat transport mechanism from the guide tube to the leadscrew. Figure 2 shows a representation of these processes in a section of a guide tube If such a transport mechanism is not very efficient, the shield provided by the guide tube can be effective and a large temperature difference between the leadscrew and the fluid temperatures in the upper plenum may exist. Further analyses were performed to test the hypothesis that the guide tube acts as a shield.

Guide Tube Model

To examine the potential shielding that the guide tube could provide, a simple model of the guide tube was developed. The model included the effects of convection and radiation heat transfer between the guide tube and the steam in the upper plenum. The model assumed the primary transport mechanism in the enclosure formed by the guide tube and the leadscrew is the recirculating flow set up by a temperature difference between these two components. The effects of radiation between the guide tube and leadscrew were also included. The following steps were used in the simple model to evaluate the temperature of

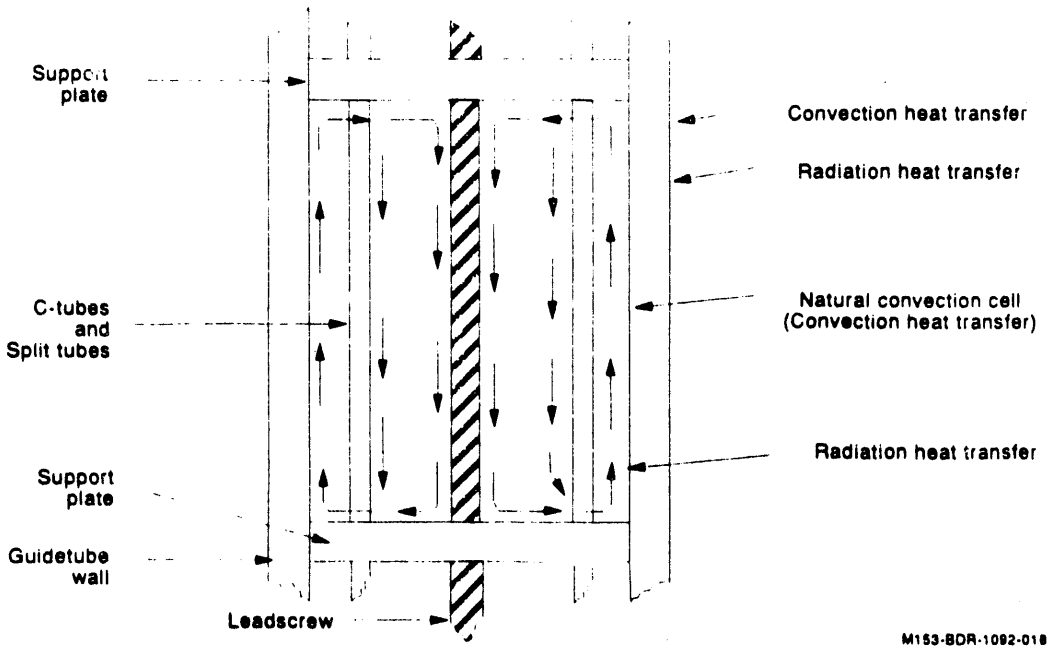

Figure 2. Guide tube representation showing heat transfer processes.

the leadscrew. It should be pointed out that the recirculating flow velocity within the cell, the fluid temperature, the leadscrew temperature, and the guide tube temperature are all known at the beginning of a time step.

a) Heat Transfer Outside The Guide Tube: The model included convection between the high temperature gas in the upper plenum and the outer surface of the guide tube. Based on the upper plenum fluid conditions, the optically thick approximation for combining convection and radiation was found to be appropriate. Consequently, radiation was included through use of an effective Prandtl Number. Use of an effective Prandtl Number is recognized to only approximate the effects of radiation but is consistent with the lack of detailed information on the surface conditions, fluid temperatures, and fluid constituents. The natural circulation velocity in the upper plenum was calculated by SCDAP/RELAP5 [3] to be approximately 0.5 m/s upward flow near the H8 leadscrew and 0.2 m/s downward flow near the B8 leadscrew. Similar natural circulation velocities were also obtained in MELPROG and FLOW3D simulations of TMI-2 [4]. The vapor flow outside the guide tube was treated as flow over a flat plate at zero incidence. Reynolds numbers were calculated which showed that the flow can be considered laminar. The actual vapor temperatures at these locations are unknown, so these temperature were varied parametrically.

The average heat transfer coefficients (at 1000 psia) outside the guide tube were calculated over a range of temperatures and locations. Using the maximum heat transfer coefficient calculated, (117 W/m^2 K), the Biot number based on the thickness of the guide tube can be found to be about 0.04. This Biot number is small enough such that the lumped capacity approximation can be applied to the guide tube wall.

b) Heat Transfer Inside The Guide Tube: Given the recirculating flow velocity within the guide tube based on the previous time step, the heat transfer coefficient on any surface in the enclosure can be found by a procedure similar to that used for the outside of the guide tube. Convection was approximated as laminar flow over a flat plated. However, the heat transfer coefficient was averaged over the cell's height and the Prandtl Number dependance was doubled to reflect this averaging process. Radiation was included using the optically thick approximation.

c) Heat Transfer To The C-Tubes, Slotted Tubes And Leadscrew: Heat transfer to the C-tubes and the slotted tubes is also similar to that between the recirculating steam and the leadscrew. The Biot number for these tubes is very small compared to unity and the maximum Biot number for the leadscrews is estimated to be about 0.10. Consequently, the lumped capacity approximation can also be applied to the C-tubes, the split tubes, and the leadscrew.

d) Temperatures: Once all of the heat fluxes were known, the change in temperatures after a time step dt was found by an energy balance for each component using the lumped capacity approximation. Fluid temperatures at each point of the flow were also determined.

e) Buoyancy Term: The buoyancy term in the momentum balance was calculated by an integration over the height of the cell.

f) Friction Term: The total frictional resistance of the flow can be found by integrating the surface shear stress over the height of the cell. The terms containing friction can be calculated using the geometry of the guide tubes and leadscrew. The friction coefficient, c_f, is modeled as a function of the Reynolds Number (Re_H) of the upflow and downflow by

$$\overline{c_f} = 1.328/\sqrt{Re_H} \qquad (1)$$

Such a friction coefficient accounts only for flow parallel to the inner tubes and lead screw. To account for the resistance caused by cross-flow at the top and bottom of the cell, the friction coefficient was determined by assuming that the cross-flow velocity at the top and bottom of the enclosure is the same as the recirculating velocity to yield

$$\overline{C_f} = \frac{1.328}{\sqrt{Re_H}} + \frac{32}{\pi}\frac{A_f}{A_w}\frac{D_R}{D_i}\left[1+\frac{10}{Re_{D_R}^{2/3}}\right] \quad (2)$$

Where A_f is the cross sectional flow area, A_w is the total wall surface area within the cell, D_R is the effective diameter of the C-tubes and split tubes, D_i is the inside diameter of the guide tube, and Re_{D_R} is the Reynolds number for the flow across the top and bottom of the cell. For the remainder of this paper, solutions obtained with the friction coefficient in Equation 1 will be referred to as the "low friction" cases while those obtained with Equation 2 will be referred to as the "high friction" cases. These "low" and "high" friction cases are estimates of lower and upper bounds of friction encountered by the recirculating flow in the enclosure.

g) Flow Velocity: The flow velocity after a time step dt can then be found by applying the buoyancy force and friction force to the mass of recirculating fluid in the cell. Once this velocity has been updated, one can go back to step a) to begin a new time step.

Calculations Performed

The following two approaches were taken in the application of the simple model for assessment of the shielding effect of the guide tube.

1. Parametric calculations were performed to examine the relationship between the steam temperature in the upper plenum and the leadscrew temperatures deduced from the TMI-2 leadscrew material samples as described in Reference 5. The steam temperature calculated in this fashion can be compared with that predicted by the codes to detect any inconsistency.

2. The upper plenum steam temperature that was calculated by MELPROG and FLOW3D (see Reference 4) is used to calculate the leadscrew temperature. The leadscrew temperatures calculated by the simple model were compared with those obtained by metallurgical examinations in Reference 5 to evaluate whether the large temperature difference between the upper plenum steam and the leadscrew is reasonable.

Results

Prior to performing calculations with the simple model, sensitivity calculations were performed to examine the effects of various combinations of time step, spatial discretization and external steam temperature. An oscillating flow velocity which damped out after about 200 seconds was calculated inside the tube. The oscillations were determined not to be a result of numerical instability. Whether these oscillations actually occurred during the TMI-2 accident is not known, but in the calculation they are of short duration compared to the time frame of the accident and would not be

expected to significantly affect the calculated temperatures. The sensitivity calculations on friction factor effects showed the circulation velocity in the guide tube was about forty percent higher with the low friction case but the effect on temperature was not as large. For example, the time it took for the leadscrew to reach 800K was about 52 min. at low friction and 57 min. at high friction, a difference of only ten percent.

Estimation of TMI-2 Upper Plenum Fluid Temperatures

The actual temporal variation of the steam temperature outside the guide tube is an unknown for the TMI-2 accident. A SCDAP/RELAP5 simulation of a Surry station blackout [3] indicated that, for a 40 minute period of natural circulation, the temperature of the fuel cladding at the top of the fuel assembly rises almost linearly. As an approximation, a linear variation of steam temperature outside the guide tube can also be assumed for TMI-2 during the period of natural circulation (139 min to 174 min). Between 110 and 139 minutes, however, the steam temperature near the top of the upper plenum is expected to rise more slowly because cladding oxidation has not begun and steam is escaping through the surge line and thus may not readily reach the top of the upper plenum. If we assume that the steam temperature near the top of the upper plenum varies parabolically with time from 110 min. to 139 min. and linearly from 139 min. to 174 min., only the maximum temperature at 174 min is needed to completely characterize the steam temperature over the excursion between 110 and 174 min.

$$\frac{T_s - 560K}{T_{max} - 560K} = \begin{cases} \dfrac{t'^2}{2871} & t' = t - 110 < 29\,min \\ \dfrac{2t' - 29}{99} & t' = t - 110 > 29\,min \end{cases} \qquad (3)$$

The assumed steam temperature's temporal variation shown in Equation 3 is only an approximation that does not account for large scale, rapid cladding oxidation. Another temporal distribution can be obtained by examining the maximum core temperature calculated for TMI-2 by SCDAP/RELAP5 [7]. Assuming that the steam temperature follows the same pattern it can be approximated by

$$\frac{T_s - 560K}{T_{max} - 560K} = \begin{cases} 7.532E\text{-}03 \cdot t' & 0\,min < t' < 47\,min \\ 6.460E\text{-}02 \cdot t' - 2.6822 & 47\,min < t' < 57\,min \\ 1.0 & 57\,min < t' < 64\,min \end{cases} \qquad (4)$$

Given a maximum steam temperature, either Equations 3 or 4 can be used to find the steam temperature as a function of time. This steam temperature then can be used to calculate the leadscrew temperature. A plot of the dimensionless steam temperatures defined by Equations 3 and 4 are shown in Figure 3.

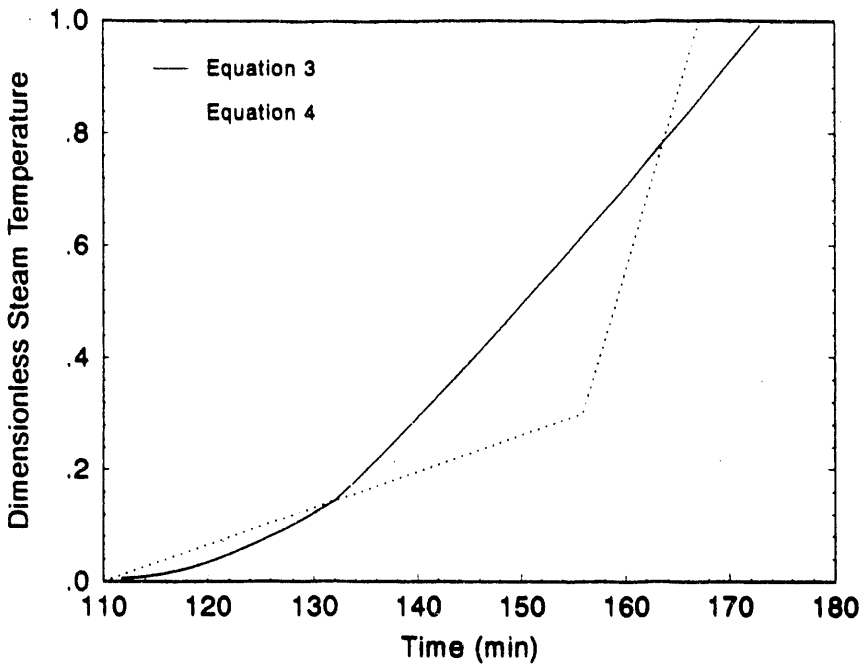

Figure 3. Assumed dimensionless steam temperatures in the upper plenum..

Equations 3 or 4 can be used as input to the simple model to calculate the leadscrew temperature as a function of time. The maximum leadscrew temperature will be the temperature calculated by the simple model at 174 min. Figure 4 shows the maximum B8 leadscrew temperature as a function of maximum steam temperature using both Equations 3 and 4. Using the maximum temperature experienced near the top of the B8 leadscrew (723 K ± 28 K) deduced in Reference 5, Figure 4 yields maximum steam temperatures of 1289K ± 91K and 1424K ± 100K using Equation 3 and 4 respectively. Using the same approach as was used for the B8 leadscrew, the maximum steam temperatures for the top of the H8 leadscrew were 1385K ± 151K and 1528K ± 175K using Equations 3 and 4 respectively.

Due to the uncertainty in the temporal variation of the steam temperature in the upper plenum, the calculated maximum steam temperatures may not represent the actual temperatures. However, they do indicate that the upper plenum steam temperature can be much higher than the maximum temperature experienced by the leadscrews. Even though the B8 leadscrew's temperature is higher than that of the H8 leadscrew (723K vs 666K) the steam temperature is found to be slightly lower. This is due to the higher heat transfer coefficient between the steam and the guide tube that exists for the B8 leadscrew. A point near the top part of the upper plenum in the center channel is at the trailing edge of the up flow while the same point in the outer channel will be near the leading edge of the returning down flow. This different relative location with respect to the flow results in a higher heat transfer coefficient for the outer channel (B8) compared to the center channel (H8). Moreover, a lower temperature in the outer channel is also consistent with the expected flow

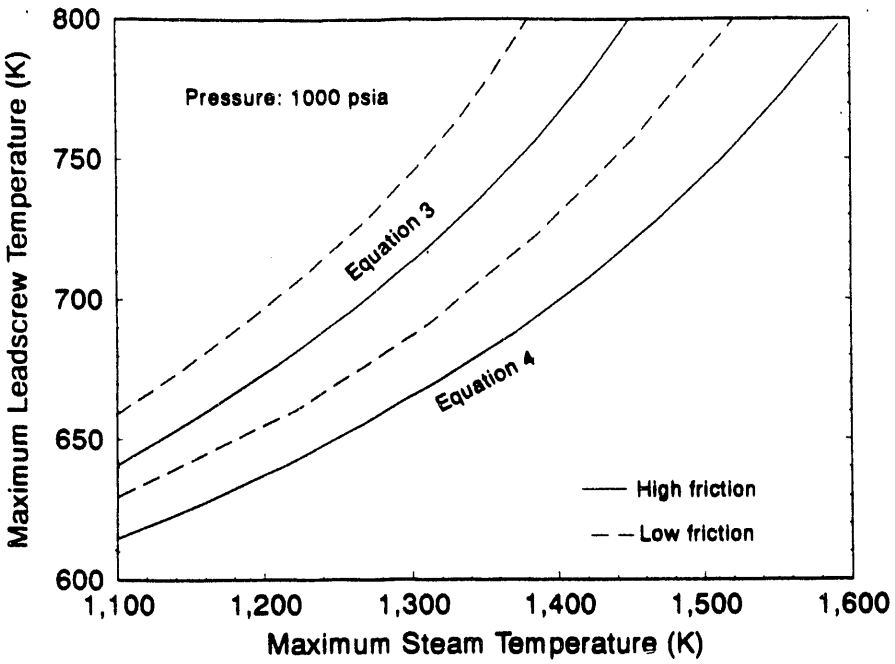

Figure 4. Maximum Leadscrew Temperature (B8).

pattern for natural circulation since the steam that goes up the center channel must lose heat to the upper head before returning to the upper plenum via the outer channel.

MELPROG and FLOW3D Temperature Profiles

Thermal-hydraulic calculations of TMI-2 using MELPROG and FLOW3D [4] indicate that the steam temperature near the top of the upper plenum is fairly uniform axially and radially. According to this calculation, the steam temperature remains at about 560K until 110 min. Thereafter, an approximately linear temperature rise is calculated until the temperature reaches about 1450K at 157 min. At this time a very steep rise brings the steam temperature to about 1800K (due to the Zirconium-Steam reaction). Because of calculational difficulties, the calculation in Reference 4 is terminated at 159 min. and further information on steam temperature in the upper plenum is unavailable after this time. However, the calculation does indicate a rate of decrease of about 1 K/s between 157 and 159 min. due to mixing with relatively cooler steam from below as the Zirconium-Steam reaction diminishes. Whether this decrease occurred during the TMI-2 accident is not known but it was included in the temperature profile. To extend the profile to 174 min., the temperature was assumed to increase with the same slope after 161.43 min. as it did prior to 157 min. Based on these assumptions, the following estimate of steam temperature was used.

$$T_s = \begin{cases} 560 + 18.94 \cdot t' & 0\,\text{min} \le t' \le 47\,\text{min} \\ 4620 - 60 \cdot t' & 47\,\text{min} < t' < 51.43\,\text{min} \\ 560 + 18.94 \cdot t' & 51.43\,\text{min} \le t' \le 64\,\text{min} \end{cases} \quad (5)$$

A similar temperature variation was produced by with SCDAP/RELAP5 calculations of the TMI-2 accident [6]. Another complication is the flow velocity in the upper plenum after 157 min. The steep rise in temperature is a result of rapid oxidation of the fuel cladding which is expected to be accompanied by a partial relocation of the core. Thereafter, the flow velocity in the upper plenum may decrease due to a change in the geometry of the core (such as the formation of blockages) and by a reduction in the boil-off rate. Therefore, heat transfer from the steam in the upper plenum to the guide tube should be maximum prior to significant core relocation. Since information on flow velocity is not available in [4] after 157 min., a conservative estimate of the leadscrew temperature will be obtained here by assuming that there is no change in the flow velocity after this time. The leadscrew temperature thus obtained is plotted in Figure 5 as a function of time. The temperatures after 157 min. are shown as dashed lines since both the natural circulation velocity and the steam temperature are expected to be lower than the values used in the calculation. From Figure 5 the temperature of the H8 leadscrew is found to be about 950K at around 170 min. This is considerably higher than the temperature deduced from metallurgical samples of the leadscrews [5] (about 700K). However, due to uncertainties in the steam temperature and natural circulation flow rate mentioned earlier, the actual leadscrew temperature must be lower than the value of 950K predicted here.

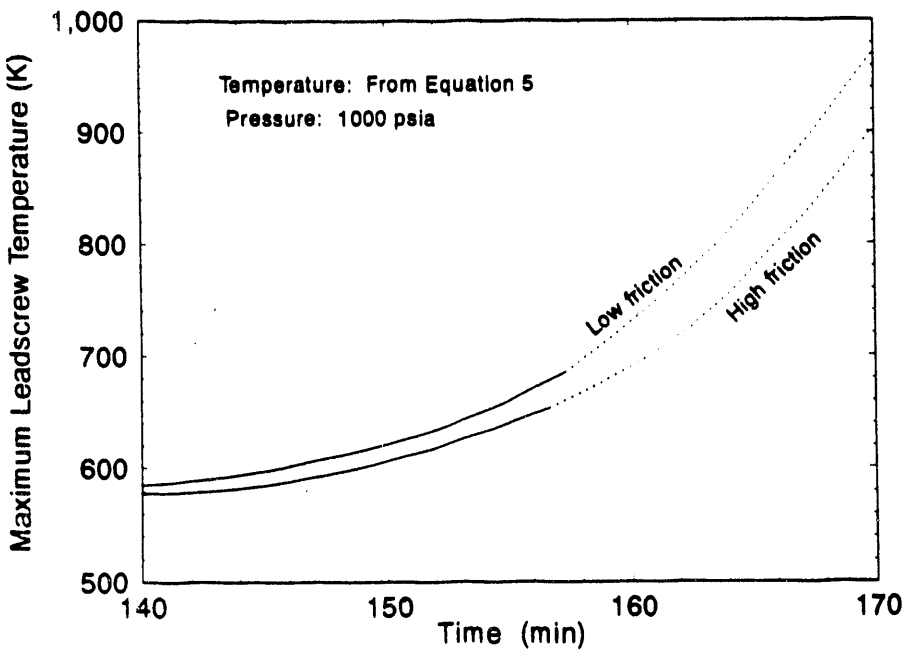

Figure 5. Leadscrew temperature - MELPROG result.

Conclusions

The following conclusions were drawn from this study on the temperature of the leadscrew recovered from the upper plenum of TMI-2.

1. Even though the actual temporal variation of the steam temperature in the upper plenum is unknown for the TMI-2 accident, results obtained in this study indicate that the maximum steam temperature can be very high (on the order of 1300K to 1500K) compared to temperatures experienced by the leadscrews (666K to 723K).

2. Using an upper plenum steam temperature calculated for TMI-2 by MELPROG and FLOW3D produces maximum leadscrew temperatures which approximate those determined by metallurgical samples of the TMI-2 leadscrews.

3. It is likely that a gravity driven recirculating flow was set up in the enclosure bounded by the leadscrew and the guide tube during the TMI-2 accident. The buoyancy term for such a flow arises from the temperature difference between the guide tube and the leadscrew.

4. Radiative exchange between the guide tube and the leadscrew may be important and must be considered as a heat transfer mechanism.

3. RELAP5/MOD3 CALCULATION OF NATURAL CIRCULATION DATA

Calculating the effects of natural circulation in the vessel, hot legs, and steam generators is very complicated owing to the complex phenomena and the multidimensional nature of the flows during the latter stages of a severe accident. The SCDAP/RELAP5/MOD3 computer code has been used to model full scale PWRs and calculate the system response during severe accidents that include natural circulation. These calculations use a specially developed nodalization of the core, upper plenum, hot legs, and steam generator plenums and tubes to simulate the multidimensional natural circulation flow behavior. During their development, coefficients in these simulated components were adjusted to ensure that the results agreed with results from detailed multidimensional simulations of PWRs.

Results from the Westinghouse natural circulation experiment apparatus provide an alternate means of evaluating the capability of SCDAP/RELAP5/MOD3 to calculate natural circulation behavior. This evaluation was performed by nodalizing the components of the Westinghouse facility using the same approach as was used for the full scale plants. Steady state experiments were selected for comparison. Experimental boundary and initial conditions were defined and specified as inputs to the model. Code modifications were made to simulate SF_6 vapor, the experiment working fluid.

Westinghouse Experiments

The objectives of the Westinghouse experiments (References 1 and 2) were to experimentally determine flow patterns, flow rates, and temperatures of natural circulation flows in PWRs during severe accidents such as a station blackout and small-break LOCA (TMLB' and S_2D) events. These experiments were conducted with a 1/7 scale model of a Westinghouse four loop PWR. Sulfur hexafluoride (SF_6) was used as the working fluid to emulate high pressure steam. Electric resistance heaters were used to simulate the core decay heat. Most of the experiments were conducted with steady cooling of the upper internals and steam generators provided by secondary side cooling water. These steady state tests allowed a more thorough investigation of the natural circulation flows. Transient tests were also conducted where the cooling was provided by the thermal storage in the model reactor structures.

Steady State Experiments

Of the 14 steady-state natural circulation tests, Tests S-6 and S-7 were chosen for modeling with RELAP5/MOD3. These two test were chosen because they had representative system conditions, including upper plenum and steam generator cooling, and the experimental data indicated that the core heating was very closely balanced with the heat removal. For some other experiments, the core heating was not in balance with the heat removal due to experimental difficulties in maintaining the cooling water at a constant inlet temperature for the duration of the test. Tests S-6 and S-7 both had core powers of 20.5 kW, but different system pressures of 240 and 315 psia, respectively.

The experimental data reported includes the fluid temperatures in the reactor vessel, hot legs, and the left steam generator tube bundle. Also, the experimental thermal boundary conditions were adequately defined and included the heat removed by the upper internals (guide tubes, upper plenum wall, and upper head) and steam generators. SF_6 mass flow rates or velocities were not measured in the experiments. Instead, they were estimated using the experimental heat removal rates, and vapor temperatures. Derived experimental flow parameters in the hot legs and steam generators were obtained as part of this study using the analytical models, methodology, and experimental data presented in the Westinghouse report (Reference 2). The derivation of these flow parameters is summarized below.

Derived Flow Parameters in the Hot Legs and Steam Generators

The experimental mass flow rate, $\dot{m}_{HL}$, in the hot leg was derived by equating the change in energy of fluid flowing through the hot leg with the heat rejected by the steam generator, q_{SG}:

$$\dot{m}_{HL} = \frac{q_{SG}}{\bar{C}_p (T_{HL,h} - T_{HL,c})} \qquad (6)$$

where $T_{HL,h}$ and $T_{HL,c}$ are the average vapor outlet and inlet temperatures in the hot leg at the steam generato junction, respectively.

The derived flow parameters in the steam generators included the left steam generator tube bundle mass flow rate and average inlet and outlet temperatures; the number of tubes carrying hot and cold flow; the average temperature in the inlet plenum mixing volume; and the fraction of flow entering the inlet plenum that is mixed with flow returning to the hot leg. Note that the experimental flow parameters were only calculated for the left steam generator because vapor temperatures were not recorded in the right steam generator inlet plenum.

The left steam generator tube bundle mass flow rate, $\dot{m}_{SG}$, was derived by equating the change in energy of fluid flowing through the steam generator with the heat rejected by the steam generator:

$$\dot{m}_{SG} = \frac{q_{SG}}{\bar{C}_p (T_{SG,h} - T_{SG,c})} \tag{7}$$

where $T_{SG,h}$ and $T_{SG,c}$ are the average fluid temperature entering and leaving the tube bundle in the inlet plenum, respectively. As was done in the Westinghouse report, measured fluid temperatures in the tubes on the inlet plenum side were sorted to find those that had hot fluid entering the bundle and those that had cooled flow returning. For Test S-6, 64 'hot' steam generator tubes and 152 'cold' tubes were estimated. The average fluid temperatures entering and leaving the tube bundle, $T_{SG,h}$ and $T_{SG,c}$, were calculated as the average temperature of the identified hot and cold thermocouple readings, respectively. The average temperature in the inlet plenum, $T_{SG,m}$, was derived using an analytical mixing model and experimental data. The mixing model results in the following expression for $T_{SG,m}$:

$$T_{SG,m} = \frac{T_{HL,h} + (\dot{m}_{SG}/\dot{m}_{HL}) T_{SG,c}}{1 + (\dot{m}_{SG}/\dot{m}_{HL})} \tag{8}$$

The mixing model was also used to estimate the mixing fractions, f_1 and f_2, which quantify the fraction of flow entering the inlet plenum from the hot leg and from the tube bundle, respectively. The flow mixing results in a lower inlet temperature to the tube bundle and raises the temperature of vapor returning to the hot leg. For symmetrical mixing, $f_1 = f_2 = f$, and the mixing fraction is defined as

$$f = 1 - (\dot{m}_{SG}/\dot{m}_{HL}) \frac{(T_{SG,h} - T_{SG,m})}{(T_{HL,h} - T_{SG,m})} \tag{9}$$

RELAP5/MOD3 Model Description

The RELAP5/MOD3 model of the Westinghouse experimental apparatus included all of the major components necessary to perform the steady state analyses. The reactor vessel, two hot legs, and two steam generators were modeled. Also, thermodynamic and thermal hydraulic properties of SF_6 vapor were obtained. Figure 6 presents the RELAP5 nodalization of the Westinghouse apparatus.

Reactor Pressure Vessel

The model of the Westinghouse experimental reactor vessel was developed analogous to that of the Surry vessel model used in earlier natural circulation analyses [3]. The core and upper plenum were divided into three radial regions. The core regions were selected so that similarly powered fuel assemblies were grouped together. The upper plenum regions were extensions of the core regions. Two-dimensional flows in the core and upper plenum were simulated by connecting the three channels at each elevation with crossflow junctions. Heat structures modeled include the reactor vessel walls, the fuel assemblies, the top nozzle assembly, the upper core plate, the upper plenum structures, and the upper head walls and internal structures. The lower plenum and upper head were also modeled. The upper head communicated with the lowest volumes in the upper plenum via the modeled communication tube flow paths. (In a reactor, this flow path is provided by the clearances in the control rod guide tubes.)

The core axial form pressure loss coefficients were calculated by the code for the specified geometry. The radial form loss coefficients could not be calculated explicitly by the code because the three channel radial nodalization oversimplified the crossflow geometry between adjacent fuel assemblies. Therefore, assumed radial form loss coefficients were specified as input. Also, the loss coefficients for the core/upper plenum junctions were not calculated with the code because the complex geometry of this junction was not characterized well enough to model accurately. (This junction includes the top nozzle assembly and the upper core plate.) Therefore, the assumed loss coefficients at the junction between the core and the upper plenum were specified.

The upper plenum's internal structures included the control rod guide tubes, communication tubes, and support columns. Additionally, the upper plenum wall enclosed these internal structures. The axial and crossflow loss coefficients for flow between adjoining upper plenum volumes were not known and assumed values were used for all these junctions. Also, during the experiments, cooling water flowed through tubing attached to the outside surface of the upper plenum wall and additional cooling water recirculated through tubing attached to the inside of the guide tubes. This cooling water entered the guide tubes through a manifold system located in the upper head. The heat removed by these cooled structures was modeled by specifying surface heat fluxes. The surface heat fluxes were determined by dividing the heat removed through the cooling systems by the structure's surface area.

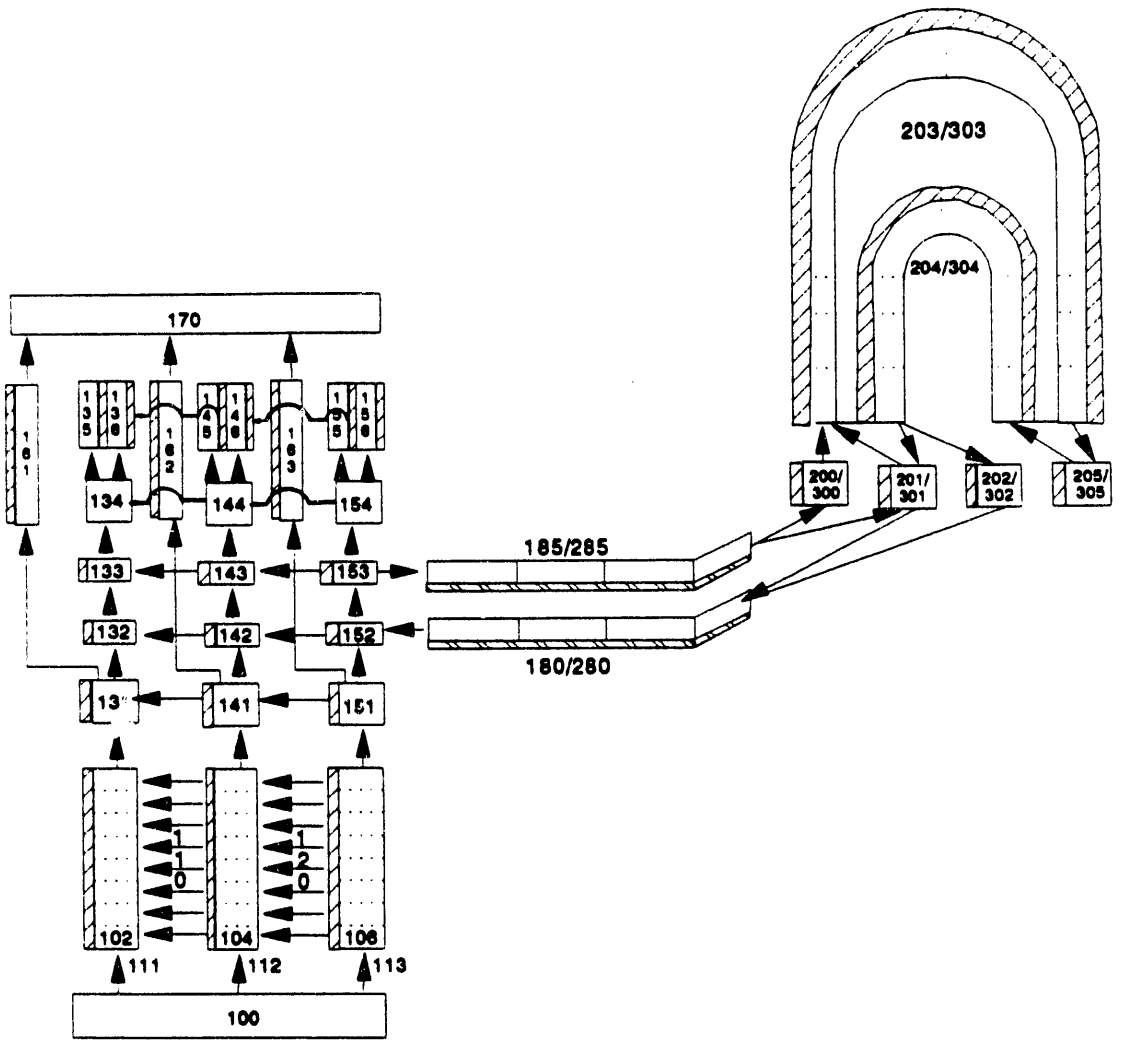

Figure 6. RELAP5 nodalization of the Westinghouse experimental natural circulation reactor pressure vessel, hot legs, and steam generators.

Hot Legs

Both hot leg pipes were modeled. The hot leg models were identical and included both the fluid volume and the metal structures. The piping was assumed to be adiabatic on the outer surface. In order to model the countercurrent flow in the hot legs, the hot leg was divided into top and bottom flow paths. The shear loss at the countercurrent flow interface was approximated by assuming the interface acted as a very rough surface with a wall roughness of 9 mm. For comparison, the surface roughness of the pipe wall was specified as 5×10^{-6} m. An equivalent wall roughness for each hot leg volume was then defined as a surface area weighted average of the interface roughness and the pipe wall roughness.

Steam Generators

The steam generator model included the tube bundle, the tube sheet, the inlet and outlet plena, the inlet channel head and flange, and the secondary side cooling water system. The left and right steam generators were modeled identically except for the secondary side cooling water inlet conditions. The metal masses associated with the steam generator walls and internals were modeled, with the outer surface of the steam generators assumed to be adiabatic. The steam generator inlet plenum was divided into three volumes. A mixing volume in the middle connected to the flows entering and leaving both the hot leg and the steam generator tubes. The volumes on either side of the mixing volume passed hot and cold vapor directly to the steam generator and hot legs, respectively, without mixing with the other fluid in the inlet plenum. Two sets of steam generator tubes connect the inlet and outlet plena. The number of tubes representing hot and cold flow tubes were derived from the Westinghouse experimental temperature data.

SF_6 Vapor Properties

For the modeled high pressure Westinghouse experiments, the system conditions were such that the SF_6 vapor properties deviated a considerable amount from ideal gas property relations. Because of the ideal gas property inaccuracies, non-ideal gas property models for SF_6 vapor were developed and implemented in the RELAP5/MOD3 code calculations. These models were developed for the specific volume, v, the coefficient of thermal expansion, β, isothermal compressibility, κ, and heat capacity at constant pressure, C_p. The non-ideal property models were obtained using a five coefficient Martin-Hou type equation of state and thermodynamic relations [8].

Analyses

An analytical simulation was performed for the Westinghouse steady state Test S-6 using the RELAP5/MOD3 computer code. Analytical results were obtained and are presented for the core and upper plenum, the two hot legs, and the two steam generators. These results include the SF_6 vapor temperatures, the mass flow rates, the heat added and removed, and the flow parameters derived in the Westinghouse experiments. Finally, some of the uncertainties and limitations of the analysis are described.

Procedure

The analysis consisted of specifying the experimental boundary and initial conditions. The calculation was run for 10,000 seconds which assured steady state results. The form loss coefficients in the steam generator inlet plenums were obtained from a benchmark calculation using Test S-7 data. In that calculation, the junction loss coefficients and flow areas for the inlet plenum volumes were adjusted until the mass flow ratio and mixing fractions, f_1 and f_2, matched the correlated experimental data for Test S-7.

Natural Circulation Flow in the Core and Upper Plenum Results

The available experimental data for the core and upper plenum consisted of vapor temperatures, core power, upper plenum cooling rates, and system pressure. Vapor flow rates and velocities were not measured in the experiments. Nevertheless, an averaged temperature distribution in the core and upper plenum was derived from the recorded experimental vapor temperatures. Figure 7 presents the experimental average temperature distribution and the RELAP5 calculated temperature distribution for Test S-6. The experimental average temperatures were obtained by first locating the position of each thermocouple relative to the RELAP5/MOD3 defined control volumes. Then, an arithmetic average of the thermocouple readings assigned to each control volume was calculated. Control volumes that did not contain a thermocouples were left blank in the distribution diagram. The average vapor temperature in the left and right hot legs at the reactor vessel junction are also shown in this Figure. The upper temperatures are for the hot flow leaving the reactor vessel and the lower temperatures are for the returning cooled flow. In the experiments, the vapor temperatures in each stream changed along the length of the hot leg because of heat transfer and mixing of the two counterflowing streams. Recorded temperatures at the steam generator end of the hot leg are not depicted here but are presented later with the hot leg results.

The observed and calculated temperature distributions are the result of the recirculating flow in the core and upper plenum. In the core there is a radial temperature distribution with higher temperatures in the center and lower temperatures at the periphery. The axial distribution governs the recirculating flow. At the core periphery, the vapor temperature increases as the flow travels down through the core and is heated up. In the center channel, the vapor heatup continues and drives the flow up through the core. In the middle channel, the axial temperature distribution is somewhat more complicated due to the recirculating flow in the core. The maximum temperature is seen about half way up the channel with much cooler temperatures above this location. This is due to a combination of two phenomena. First, high temperatures occur half way up the channel because flow stagnated in the recirculating pattern is heated to higher temperatures. Secondly, lower temperatures occur at the top of the core due to cooler vapor in the upper plenum flowing into the core.

In the upper plenum, the radial temperature distribution is similar to that in the core with hotter vapor rising in the center channel and cooler fluid descending at the plenum periphery. The axial temperature distribution in the upper plenum is reversed to that in the core. As the fluid rises in the center channel, the vapor decreases in temperature as energy is transferred to the water cooled guide tube structures. The vapor temperature continues to decrease as it turns and descends down the periphery of the plenum.

A comparison of the calculated temperature distribution with the derived experimental average temperatures reveals that the model overpredicts the experimental values in the core region, underpredicts in the upper plenum and head, and yields mixed results in the communication tubes. Quantitatively,

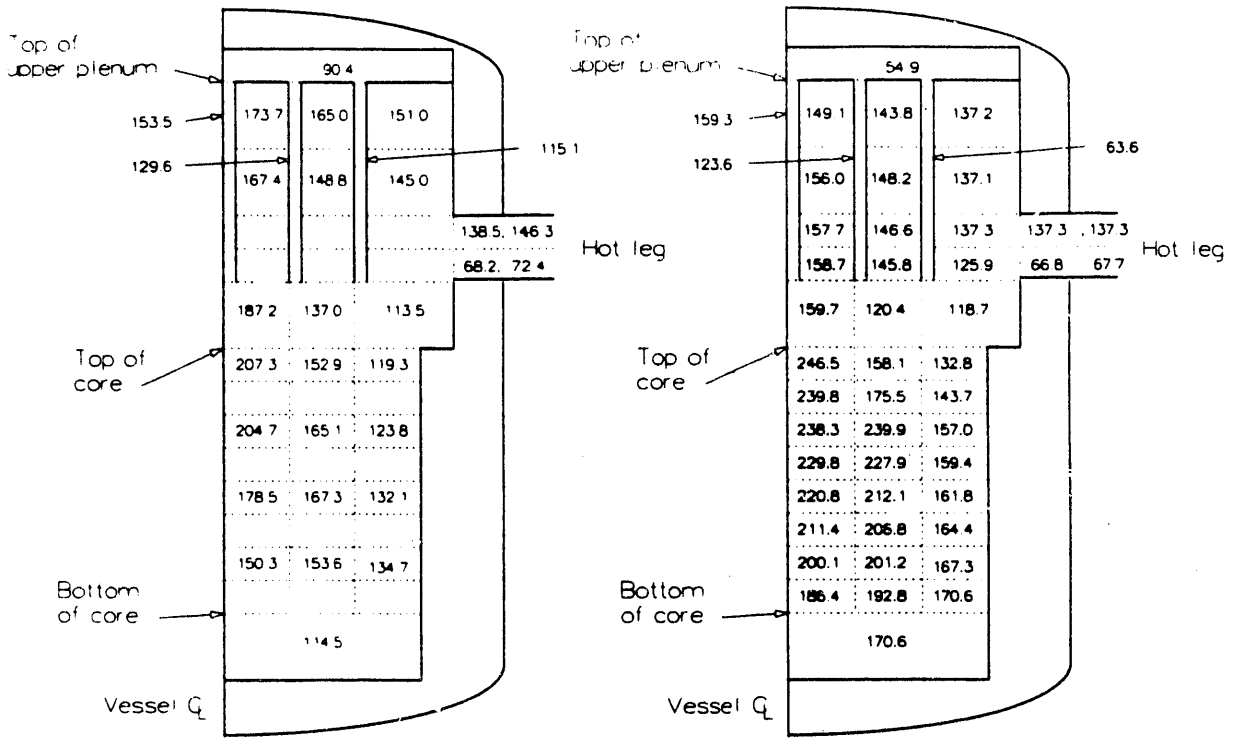

Experimental **Calculated**

Figure 7. Experimental and RELAP5 calculated SF_6 vapor temperatures (°C) in the core and upper plenum for Test S-6.

the maximum temperature is found at the top of the core in the center channel and calculated as 246.5°C. The experimentally averaged maximum temperature was also seen at this location and was 207.3°C. This is approximately 39°C lower than the calculated value. The minimum temperature is found in the upper head, where the vapor is cooled by the cooling water manifold located there. The calculated vapor temperature in the upper head was 54.9°C. In the experiment, the average vapor temperature in the upper head was 90.4°C or approximately 35°C greater than the calculated value. In the upper plenum, the lowest vapor temperature is found at the bottom of the outer channel where the cooled flow returning from the hot leg is mixed with the flow descending from the upper plenum and cool vapor returning from the upper head via the communication tubes. The calculated minimum upper plenum temperature was 118.7°C. Experimentally, the minimum upper plenum temperature was also observed in this region with an average value of 113.5°C. This is approximately 5°C lower than the calculated value.

One probable cause-of the overpredicted core temperatures and underpredicted upper plenum temperatures are too large of values for the loss coefficients at the core/upper plenum junctions. This causes a flow restriction between the core and the upper plenum and results in a longer transit time through the

core and upper plenum. The longer transit times in the core yields greater vapor temperatures and in the upper plenum results in lower vapor temperatures. The core/upper plenum junction loss coefficient was assumed to be 40.0 in the calculation. A theoretical evaluation of this loss coefficient was not made because the geometry of the upper core plate and top nozzle assembly was complex and not well characterized.

The upper head vapor temperature is underpredicted most likely due to an overestimation of the heat removed by the cooling water manifold. The vapor flow exiting the upper head and returning to the upper plenum via the outer channel communication tubes is also underestimated because of the underestimated upper head vapor temperature. The heat removed by the cooling water manifold was not reported explicitly in the experimental results, but was included in the total heat removed via the upper plenum guide tube cooling. The model assumed that the heat flux removed by the manifold and guide tubes was equal. However, the results indicate that this assumption is incorrect. A better comparison of the upper head results could be obtained by adjusting the specified heat flux. In any case, the vapor circulation through the upper head accounts for less than 5% of the heat removed from the core and does not significantly affect the overall problem.

Flow Pattern Distributions. The calculated average SF_6 vapor mass flow rate and velocity vectors in the core and upper plenum for Test S-6 are presented in Figure 8. Comparison with experimental data was not possible because no mass flow rates or velocities were measured in the experiments. The core and upper plenum vector diagrams confirm the recirculation flows indicated by the temperature distribution. The recirculating mass flow rate in the upper plenum is approximately 2.6 times that in the core, with mass flow rates approximately, 0.54 and 0.20 kg/s, respectively. By comparison, the mass flow rate recirculating through the upper head is only 0.05 kg/s and that through each hot leg loop is 0.045 kg/s, on average.

The velocity vector diagram shows a flow pattern similar to that of the mass flow rate diagram. In the core, the maximum velocity occurs in the outer channel and is approximately 0.16 m/s. In the upper plenum, the maximum velocity occurs in the center channel and is 0.30 m/s. The velocity in the communication tubes is much higher than in other regions of the upper plenum because of the relatively small cross-sectional flow area of the tubes. The calculated velocity in the center channel communication tube was 1.5 m/s.

Countercurrent Hot Leg and Steam Generator Flow Results

Derived flow parameters in the hot legs and steam generators are presented and compared with the experimental results in Table 1. The hot leg results include the vapor temperatures and mass flow rates. The hot and cold vapor temperatures are overpredicted, on average, by less than 4% and 5%, respectively. The hot leg temperature differences are overpredicted by 4%, on average, and the mass flow rates are underpredicted by approximately, 4%.

The steam generator heat removal rates compare quite well with the

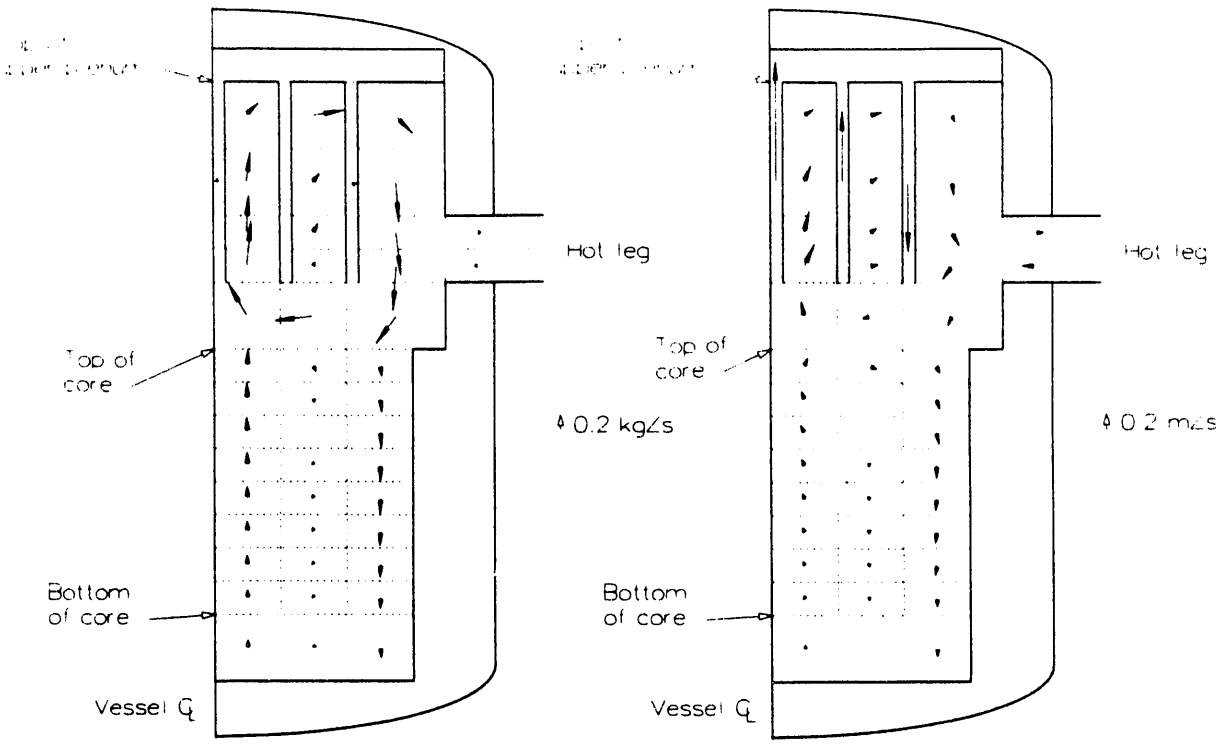

Figure 8. Calculated SF_6 vapor mass flow rate and velocity vectors in the core and upper plenum for Test S-6.

experimental results and deviate by approximately 1%, on average. The tube bundle mass flow rate is underpredicted by approximately 1%. The tube bundle entrance and exit temperature are underpredicted by 1.4% and 3.8%, respectively, and the steam generator temperature difference is within 2% of the experimental value. Finally, the mixing volume temperature is within 2% of the experimental value.

While most of the hot leg and steam generator results are predicted to within ~8% of the experimental data, whether this agreement is adequate or not depends upon how sensitive the core condition and reactor coolant system failure time and location are to the hot leg and steam generator flow parameters. Determination of the various system sensitivities is beyond the scope of this study and would be better suited to examination with a full plant sensitivity study. However, during the benchmarking of calculated the results with Test S-7 data it was observed that the mass flow rates and vapor temperatures in the hot legs are strongly dependent upon the steam generator flow parameters including the heat removed in the steam generator, the inlet plenum mixing fractions, and the ratio of the steam generator mass flow rate to the hot leg flow rate. It was also observed that changes in the core and upper plenum system modeling had only a small affect on the hot leg and steam

Table 1. Experimental and RELAP5 calculated natural circulation flow parameters in the hot legs and steam generators for Test S-6.

	Experiment		Prediction		Percent Error	
Hot Leg	Left	Right	Left	Right	Left	Right
$T_{HL,h}$ (°C)	129.7	134.9	137.3	137.3	5.9	1.8
$T_{HL,c}$ (°C)	65.5	63.4	67.7	66.8	3.4	5.4
$T_{HL,h} - T_{HL,c}$ (°C)	64.2	71.5	69.6	70.5	8.4	-1.4
m_{HL} (kg/s)	0.0467	0.0461	0.0445	0.0451	-4.7	-2.2
Steam Generator						
q_{SG} (kW)	2.43	2.67	2.49	2.55	2.5	-4.5
m_{SG} (kg/s)	0.0919	NA	0.0907	0.0891	-1.3	
f_1	0.85	NA	0.89	0.89	4.7	
f_2	0.85	NA	0.89	0.89	4.7	
$T_{SG,h}$ (°C)	77.5	NA	76.4	75.9	-1.4	
$T_{SG,c}$ (°C)	44.5	NA	42.8	40.9	-3.8	
$T_{SG,h} - T_{SG,c}$ (°C)	33.0	NA	33.6	35.0	1.8	
$T_{SG,m}$ (°C)	73.2	NA	74.5	74.0	1.8	

NA Data was not obtained in the experiments.

generator flow parameters. For example, the temperature of the hot flow entering the top of the hot leg from the upper plenum is dependent upon the vapor temperature and mixing that occurs in the periphery of the upper plenum. However, changes in the upper plenum modeling had little affect on these. If it is desired to reduce the uncertainty in the hot leg and steam generator modeling, most likely enhanced modeling of the ex-vessel systems would be required. Possible enhancements would included increased nodalization, mechanistic models of the countercurrent hot leg flow that would include heat and mass transfer between the two streams, and three dimensional flow models of the steam generator inlet plenum.

Uncertainties and Limitations

One uncertainty in the analysis that has not been addressed is what affect the model nodalization has on the results. Also, some of the model loss coefficients are uncertain. These include the crossflow loss coefficients in the upper plenum and core; the axial loss coefficients for the core/upper plenum junctions; and loss coefficients between the steam generator inlet plenum, hot leg, and steam generator tube volumes. Some of these loss coefficients, such as the crossflow losses in the core, could be determined explicitly by increased nodalization, but there is not sufficient information to quantify the others.

There is also uncertainty in the steam generator inlet plenum mixing model. Specifically, the derived mixing fractions assume perfect mixing and no heat transfer between the defined flow streams in the inlet plenum. The validity of this simplification and the sensitivity of the inlet plenum mixing to it are unknown. The experimental derived steam generator and hot leg mass flow rates also have unquantified uncertainties. These flow rates are derived from averaged hot leg and steam generator inlet and outlet temperatures. Deviations as high as 10% occur in the experimental temperatures used in calculating the averages.

Finally, the RELAP5 model can only simulate three-dimensional flows with a simplified two-dimensional approximation. Three-dimensional flows have been experimentally observed to occur in the core, upper plenum, hot legs, and steam generator inlet plena. Also, the hot leg model does not account for heat and mass transfer between the counter flowing streams. Experimentally, the top hot leg flow stream decreased in temperature as it traveled from the reactor vessel to the steam generator inlet plenum and the bottom flow stream increased in temperature as it returned to the reactor vessel. The temperature change was approximately 5 to 10°C in both directions. In the current hot leg model, the vapor temperature remains constant as it passes from the reactor to the steam generator and vice versa.

Conclusions

This RELAP5/MOD3 model analysis of the Westinghouse natural circulation experiment system has demonstrated:

1. Predicted SF_6 vapor flow rates and temperatures in the hot legs and steam generators compare reasonably well with the experimental data. The code tended to overpredict hot leg vapor temperatures by up to 14% and underpredicted steam generator vapor temperatures by up to 4%.

2. Vapor temperatures in the core are overpredicted and in general are underpredicted in the upper plenum. Qualitatively the temperature distributions compare well with the experimental data. One possible explanation for the quantitative differences is due to an overestimated loss coefficient for the upper core plate and top nozzle assembly which separate the core from the upper plenum. This high resistance restricts the circulation between the two regions, increases the transit times in each region, and results in hotter vapor temperatures in the core and cooler temperatures in the upper plenum. An additional calculation is planned to evaluate the sensitivity of the temperature to this resistance. Another possible cause of errors is the three dimensional nature of the flows and the simplifications associated with simulating them with a one dimensional code.

3. The vapor flow rates and temperatures in the hot legs are strongly coupled with the steam generator tube flow rates and the steam generator inlet plenum mixing. However, the hot leg and steam generator natural circulation loops are weakly coupled with the core and upper plenum flow

conditions. Therefore, uncertainties in system modeling or calculated behavior in the core and upper plenum have only a small affect on the hot leg and steam generator results.

It would appear that the two pipe model of the hot leg adequately represents the simple countercurrent flow behavior. The coupling between the steam generator and the hot leg piping appears to be adequate. However, the effect of uncertainties in this coupling on full scale plant calculations was not investigated.

4. REFERENCES

1. W. A. Stewart, A. T. Pieczynski, and V. Srinivas, "Experiments on Natural Circulation in a Pressurized Water Reactor Model for Degraded Core Accidents." Final Report, EPRI Project No. RP2177-5, 1990.

2. W. A. Stewart, A. T. Pieczynski, and V. Srinivas, "Experiments on Natural Circulation in a Pressurized Water Reactor Model With High Pressure SF_6." Draft EPRI Report, 1990.

3. P. D. Bayless, "Analyses of Natural Circulation During a Surry Station Blackout Using SCDAP/RELAP5," NUREG/CR-5214, 1988.

4. J. N. Lillington, A. J. Lyons, I. M. Lovely, "Thermal-Hydraulic Calculation in TMI-2 Accident Analysis," Reactor Systems Analysis Division, AEE Winfrith, Report No. AEEW-R 2434, January 1989.

5. K. Vinjamuri, D. W. Akers and R. R. Hobbins, "Examination of H8 and B8 Leadscrews From Three Mile Island Unit 2," GEND-.NF-052, Sept. 1985.

6. J. E. Obrien, "Effects of Hydrogen Generation on Severe Accident Natural Circulation", Proceedings of the Nineteenth Water Reactor Safety Information Meeting, NUREG/CP-0180, March 1992.

7. D. W. Golden and N. Ohnishi, "SCDAP/RELAP5 Demonstration Calculation of The TMI-2 Accident," EG&G Report, EGG-TMI-8473, March 1989.

8. W. H. Mears, E. Rosenthal, and J. V. Sinka, "Physical Properties and Virial Coefficients of Sulfur Hexafluoride," J. Phys. Chem., 73, 7, July 1969, pp. 2254-2261.

DISCLAIMER

END

DATE
FILMED
3/16/93